accepted by *ApJ Letters* on Feb. 1, 2007

A Mass Function Constraint on Extrasolar Giant Planet Evaporation Rates

W. B. Hubbard and M. F. Hattori

Lunar and Planetary Laboratory, The University of Arizona, Tucson, AZ 85721-0092

hubbard@lpl.arizona.edu, makih@lpl.arizona.edu

and

A. Burrows and I. Hubeny

Department of Astronomy, The University of Arizona, Tucson, AZ 85721-0065

burrows@as.arizona.edu, hubeny@as.arizona.edu

ABSTRACT

The observed mass function for all known extrasolar giant planets (EGPs) varies approximately as M^{-1} for mass M between ~ 0.2 Jupiter masses (M_J) and $\sim 5\ M_J$. In order to study evaporation effects for highly-irradiated EGPs in this mass range, we have constructed an observational mass function for a subset of EGPs in the same mass range but with orbital radii < 0.07 AU. Surprisingly, the mass function for such highly-irradiated EGPs agrees quantitatively with the M^{-1} law, implying that the mass function for EGPs is preserved despite migration to small orbital radii. Unless there is a remarkable compensation of mass-dependent orbital migration for mass-dependent evaporation, this result places a constraint on orbital migration models and rules out the most extreme mass loss rates in the literature. A theory that predicts more moderate mass loss gives a mass function that is closer to observed statistics but still disagrees for $M < 1\ M_J$.

Subject headings: molecular processes — planetary systems

1. Introduction

The rate of mass loss during evolution of highly-irradiated EGPs has important implications for our understanding of the origin of these unanticipated objects. The principal purpose of this *Letter* is to show that enough such objects have now been detected to permit construction of a mass function for highly-irradiated EGPs, in the mass range where strong evaporation effects had been predicted (Baraffe et al. 2004). The derived mass function shows no evidence for mass loss; its resemblance to the mass function for all observed EGPs may instead be a constraint on migration theories.

Our analysis (Hubbard et al. 2006) is based on a single dimensionless parameter ϵ which represents the efficiency of the mass loss process:

$$\epsilon = \Phi E_{B,mod}/S_*, \tag{1}$$

where Φ is the flux of escaping molecules (number per unit area per unit time), $E_{B,mod}$ is the gravitational binding energy of a molecule to the planet, as modified by the tidal potential, and S_* is the bolometric stellar flux (energy per unit area per unit time) at the planet's orbital distance, for a main-sequence star of solar mass and age. Hubbard et al. (2006) calculate the EGP mass-loss rate as a function of time by coupling this parameter to evolutionary models for EGPs orbiting solar-mass stars at orbital radii in the range 0.023 AU to 0.057 AU. The calculations of Baraffe et al. (2004) can be reproduced by setting $\epsilon = 10^{-4}$. A model scaled to the calculations of Watson et al. (1981), as well as to the lower limit considered by Baraffe et al. (2006), corresponds to $\epsilon = 10^{-6}$. In this paper, we use the suite of models of Hubbard et al. (2006) to investigate the cumulative effect of mass loss on an initial mass function for highly-irradiated EGPs.

2. Initial Mass Function

We assume an initial mass function $f(M, 0)$ defined as follows. The database of EGPs known in 2005 (Marcy et al. 2005) has a mass function (the mass M is multiplied in most cases by the unknown sine of the orbit inclination i) corresponding to

$$f(M, 0) \equiv dN/dM \propto M^{-1}. \tag{2}$$

Our independent fit to a slightly different database, the table of $M \sin i$ and orbital semimajor axis a for reported EGPs as given by Schneider (2006) in mid-2006, gives a similar result, $dN/dM \propto M^{-1.19}$. As discussed by Burrows et al. (2001) and Marcy et al. (2005), when one corrects the underlying function dN/dM for random orbit inclinations, the index is essentially unchanged, and for an index of -1 it is exactly unchanged.

In this paper, we define the initial mass function (IMF) for highly-irradiated EGPs somewhat differently than the IMF for stars, the latter referring to the stellar birth function. Since the majority ($\sim$ 75%) of detected EGPs have orbital radii > 0.07 AU, they cannot have suffered significant mass loss from atmospheric escape over their lifetime. We refer to the latter class as "field" EGPs. Our hypothesis is that highly-irradiated EGPs are not formed *in situ*, but are remnants of field EGPs that have migrated inward to small orbital radii during the $\sim 10^6$ to 10^7 years that the star's initial planet-forming nebula persists. Let the IMF denote the initial mass function for highly-irradiated EGPs at age $t \sim 10^6$ to 10^7 yr in a mass range $\sim 0.2\ M_J < M <\sim 5\ M_J$, when these EGPs start their atmospheric erosion. This IMF may well differ from the observed mass function for field EGPs, since the migration mechanism could have a mass dependence. One prediction of the IMF for highly-irradiated EGPs (Del Popolo et al. 2005) suggests a depletion of planets with $M > 4$ M_J but that lower-mass EGPs migrate inward readily (see also Trilling et al. (1998) and Trilling et al. (2002)). In this paper we make the provisional assumption that the IMF has the same index as the mass function for field EGPs.

Figure 1 shows our assumed IMF $f(M, 0)$ (heavy solid line), arbitrarily normalized to unity at $M = 1\ M_J$. We assume that EGPs born at $a \sim$ several to several $\times 10$ AU are deposited at smaller orbital radii $a \sim$ few$\times 10^{-2}$ AU within the first few$\times 10^6$ years of the parent star's lifetime. To map the IMF onto a time-dependent ensemble of eroding EGPs, we fix the distance from the star at one of the four standard distances studied in Hubbard et al. (2006), ranging from 0.023 to 0.057 AU. We then randomly choose an exoplanet of initial mass M_0 from the IMF and allow it to lose mass as a function of time t using either the Watson et al. (1981) or the Baraffe et al. (2004) prescription.

It is necessary to impose a low-mass cutoff to the IMF. As shown by Hubbard et al. (2006), hydrogen-rich EGPs with masses $\leq 0.2\ M_J$ and initial entropies corresponding to isolated EGPs at $\sim 10^6$ years of age, have such large radii that their atmospheres are tidally unbound (independent of the mass-loss rate), and so we restrict our analysis to $M_0 \geq 0.2$ M_J.

3. Mass Loss Models

We have synthesized time-dependent mass functions $f(M, t)$ for EGPs at the four orbital radii investigated by Hubbard et al. (2006). Figure 1 shows resulting mass functions at $t = 5$ Gyr after simultaneous mass loss and evolution of the EGP. In all cases, the mass functions are normalized to unity at $M = 1\ M_J$. For fixed total initial mass of the ensemble, all subsequent mass functions would plot below the IMF due to mass loss, with the strongest

deviations at the lowest mass. However, we renormalize the theoretical curves to 1 M_J for comparison with the observed mass function data points.

3.1. Lammer Model

We denote by "Lammer Model" the evaporation theory of Lammer et al. (2003) as incorporated in the predictions of Baraffe et al. (2004). We do not separately simulate the implications of more moderate mass-loss rates investigated in more recent publications (Baraffe et al. 2006; Alibert et al. 2006) because these are bounded by the Baraffe et al. (2004) rates and the Watson model. In agreement with the findings of Hubbard et al. (2006), 5-Gyr mass functions corresponding to the Lammer model show the strongest effect of mass loss. At the smallest orbital radius investigated, $a = 0.023$ AU, the predicted 5-Gyr mass function (solid curve) has a positive slope for the entire mass interval plotted in Fig. 1, while the IMF has a negative slope. This behavior occurs because mass loss biased to the lowest-mass EGPs rapidly depletes their larger initial numbers. Indeed, the mass function plotted is almost entirely populated by remnants of EGPs with initial masses $M_0 > 3-4\ M_J$ (see Fig. 7 of Hubbard et al. (2006)). For the largest orbital radii investigated, $a = 0.057$ AU, after 5 Gyr there *is* a peak in the mass distribution at $M \sim 2.3\ M_J$.

3.2. Watson Model

In contrast, the Watson model predicts essentially no deviation of the mass function from the IMF for $M > 1\ M_J$. However, as we see from the curves in Fig. 1, for $M < 1\ M_J$ the Watson model predicts significant deviations from the IMF, with a maximum at about one Saturn mass for $a = 0.057$ AU and at even higher masses for smaller orbital radii.

4. Observed Mass Function

The database from which we construct the mass function for highly-irradiated EGPs comprises ~ 40 objects (Table 1). These objects were selected from the list of all reported EGPs (Schneider 2006) according to the criteria $0.2\ M_J \leq M \sin i \leq 5\ M_J$ and $a \leq 0.07$ AU. We selected a central mass bin of width $0.3\ M_J$, according to $0.9\ M_J \leq M \sin i < 1.2\ M_J$, containing four objects (Table 1), with dN/dM to be normalized to unity at this bin. Bins were chosen to be of equal width to the central bin, except for the smallest-mass bin $0.2\ M_J \leq M \sin i < 0.3\ M_J$, which is of width $0.1\ M_J$, because of the cutoff at $0.2\ M_J$, and

for the largest-mass bins, 1.5 $M_J \leq M \sin i < 3\ M_J$ and 3.0 $M_J \leq M \sin i < 4.5\ M_J$, which are five times wider because of the small number of high-mass objects in the sample.

The resulting mass function is plotted in Fig. 2, with error bars determined by Poisson statistics. Also shown in Fig. 2 is the average orbital radius (in AU) of objects in the bin (number to the left of the error bar), and the average age (in Gyr) of the host stars in the bin (number to the right of the error bar).

It is remarkable that the mass function for these highly-irradiated objects is in agreement with the field IMF (see Marcy et al. (2000) for a discussion of selection bias).

5. Mass Function With $\sin i$ Factor

For comparison of the mass-loss models with observed statistics, we require a transformation of the theoretical mass function to a function of the new independent variable $M \sin i$. Let $f(M,t)$ be the mass function of an eroded ensemble of EGPs after time t. We write

$$f(M,t) = f(q/\sin i, t), \tag{3}$$

where the new independent variable $q = M \sin i$. Now holding the observed quantity q fixed, we average the ensemble of eroded EGPs over all solid angles of presentation of their orbits to the observer $d\Omega$, according to

$$g(q,t) = \int \frac{d\Omega}{4\pi} f(q/\sin i, t) = \int_0^1 d\mu f(q/\sqrt{1-\mu^2}, t), \tag{4}$$

where $d\mu = \sin i di$. As would be expected, averaging over $\sin i$ moves the maxima of the mass functions to slightly smaller masses. The resulting functions $g(q, t = 5\ \mathrm{Gyr})$ for the Watson model (curves to the left of $M \sin i = 1\ M_J$) and the Lammer model (curves to the right of $M \sin i = 1\ M_J$) are plotted in Fig. 2.

6. Conclusions

Our results strongly suggest that the mechanism for transporting EGPs to small orbital radii does not significantly change their mass function in the mass range considered here, and that unless a remarkable compensation of evaporation for migration has occurred, we have no evidence for evaporation effects. It is difficult to envision such a compensation. For example, to fit the observed mass function using the Lammer evaporation model, we would need to start with an IMF with an index ~ -3.6, but the fit would be highly sensitive to the ages of

the objects and would rapidly change with time. Instead, a parsimonious interpretation of the data would be that mass loss does not play a dominant role in even the hottest EGPs with $M > 0.2\ M_J$. If we take the observed numbers of EGPs in the two innermost mass bins to be statistically valid, even the more moderate Watson model still disagrees with the data, but certainly less decisively than does the Lammer model. However, our arguments seem to point in the direction of requiring the mass-loss parameter ϵ to be even smaller than 10^{-6}. All published theories give values higher than this number; for example Tian et al. (2005) and Yelle (2006) have $10^{-6} < \epsilon < 10^{-4}$.

We must mention some caveats. Comparison of theory with the observational database is complicated by the fact that a majority of the observed objects in the bins $0.6\ M_J \leq M \sin i \leq 1.2\ M_J$ are transiting EGPs (indicated by an asterisk in Table 1), and thus the masses in these bins are true masses without the $\sin i$ ambiguity. A more consistent mass function can be derived once we have enough transiting EGPs to construct a statistically significant mass function for them alone. Also, we have not included "Neptunes" in our analysis, although some highly-irradiated "Neptunes" do exist (Butler et al. 2004; McArthur et al. 2004; Santos et al. 2004; Lovis et al. 2006). Our assumed sharp mass cutoff at $0.2\ M_J$ is actually an approximation to a somewhat fuzzy boundary whose details depend greatly on the exact model for tidal effects and on the initial entropy of such low mass hydrogen-rich objects. Our previous analysis (Hubbard et al. 2006) confirms that such "Neptunes" cannot be Jupiter-like EGPs (i.e., predominantly hydrogen), but must have large fractions of elements with $Z > 2$. Whether nature could ever form hydrogen-rich low-mass (Neptune) EGPs is highly debatable. We eagerly await observations of transits by "Neptunes".

As more transiting EGPs are detected (and these will be predominantly highly-irradiated ones), a more definitive statistical test of orbital-migration and mass-loss theories will be possible.

This study was supported in part by NASA Grant NAG5-13775 (PGG), NASA grant NNG04GL22G, and through the NASA Astrobiology Institute under Cooperative Agreement No. CAN-02-OSS-02 issued through the Office of Space Science.

REFERENCES

Alibert, Y., et al. 2006, A&A, 455, L25

Baraffe, I., Selsis, F., Chabrier, G., Barman, T.S., Allard, F., Hauschildt, P.H., & Lammer, H. 2004, A&A, 419, L13

Baraffe, I., Chabrier, G., Barman, T.S., Selsis, F., Allard, F., & Hauschildt, P.H. 2005, A&A, 436, L47

Baraffe, I., Alibert, Y., Chabrier, G. & Benz, W. 2006, A&A, 450, 1221

Burrows, A., Hubbard, W.B., Lunine, J.I., & Liebert, J. 2001, *Rev. Mod. Phys.* 73, 719

Butler, R.P. et al. 2004, ApJ, 617, 580

Del Popolo, A., Ercan, N., & Yesilyurt, I.S. 2005, A&A, 436, 363

Hubbard, W.B., Hattori, M.F., Burrows, A., Hubeny, I., & Sudarsky, D. 2006, *Icarus*, in press

Lammer, H., Selsis, F., Ribas, I., Guinan, E.F., Bauer, S.J., & Weiss, W.W. 2003, ApJ, 598, L121

Lovis, C. et al. 2006, Nature, 441, 305

Marcy, G.W., Cochran, W.D., & Mayor, M. 2000, Protostars and Planets IV, V. Mannings, A.P. Boss, & S.S. Russell, Tucson: U. Arizona Press, 1285

Marcy, G., Butler, R.P, Fischer, D., Vogt, S., Wright, J.T., Tinney, C.G., & Jones, H.R.A. 2005, Progress of Theoretical Physics Supplement No. 158, 1

McArthur, B.E. et al. 2004, ApJ, 614, L81

Santos, N.C. et al. 2004, A&A, 426, L19

Schneider, J., The Extrasolar Planets Encyclopaedia, http://exoplanet.eu

Tian, F., Toon, O. B., Pavlov, A. A., & De Sterck, H. 2005, ApJ, 621, 1049

Trilling, D.E. et al. 1998, ApJ, 500,428

Trilling, D.E., Lunine, J., & Benz, W. 2002, A&A, 394.241

Watson, A.J., Donahue, T.M., & Walker, J.C.G. 1981, *Icarus* 48, 150

Yelle, R.V., 2006, Icarus 183, 508

Table 1. EGPs Used for Calculation of Mass Function

Planet Name	e	$(M \sin i)/M_J$	a (AU)	Star Age (Gyr)	Star Mass ($M_\odot$)
		0.2 to < 0.3 M_J			
HD 76700 b	0.13	0.197	0.049	4.52	1.0
HD 88133 b	0.11	0.22	0.047	9.56	1.2
HD 168746 b	0.081	0.23	0.065	3.75	0.92
HD 46375 b	0.063	0.249	0.0398	4.96	1.0
HD 109749 b	0.01	0.28	0.0635	10.3	1.2
		0.3 to < 0.6 M_J			
HD 149026 b*	0	0.36	0.042	5.8	1.3
HD 63454 b	0	0.385	0.0363	1.0	0.8
HD 83443 b	0.012	0.41	0.0406	2.94	0.79
HD 75289 b	0.034	0.42	0.046	4.96	1.05
HD 212301 b	0	0.45	0.0341	5.9	1.0
51 Peg b	0.013	0.472	0.0527	6.6	1.06
HD 2638 b	0	0.477	0.0436	3.0	0.93
BD −10 3166 b	0.07	0.48	0.046	4.18	1.1
HD 102195 b	0.06	0.492	0.0491	2.4	0.93
HD 187123 b	0.023	0.528	0.0426	5.33	1.06
OGLE-TR-111 b*	0	0.53	0.047	···	···
HAT–P-1 b*	···	0.53	0.055	3.6	1.12
OGLE-TR-10 b*	0	0.54	0.04162	···	···
		0.6 to < 0.9 M_J			
υ And b	0.012	0.69	0.059	2.41	1.3
HD 209458 b*	0	0.69	0.0474	4.72	1.01
TrES-1 b*	0	0.759	0.0394	2.41	0.87
HD 330075 b	0	0.76	0.043	6.21	0.95
WASP-2 b*	···	0.88	0.0307	···	···
WASP-1 b*	···	0.89	0.0382	···	···

Table 1—Continued

Planet Name	e	$(M \sin i)/M_J$	a (AU)	Star Age (Gyr)	Star Mass ($M_\odot$)
		0.9 to < 1.2 M_J			
XO-1 b*	···	0.9	0.0488	···	···
HD 179949 b	0.022	0.98	0.0443	2.05	1.24
HD 188753A b	0	1.14	0.0446	···	···
HD 189733 b*	0	1.15	0.0312	6.1	0.9
OGLE-TR-113 b*	0	1.19	0.0306	···	1.35
		1.2 to < 1.5 M_J			
TrES-2 b*	0	1.28	0.0367	···	1.08
OGLE-TR-56 b*	0	1.29	0.0225	2	1.17
OGLE-TR-132 b*	0	1.32	0.0229	> 0.7	0.78
HD 149143 b	0	1.33	0.0531	7.6	1.21
HD 86081 b	0.006	1.49	0.0346	···	1.0
		1.5 to < 3 M_J			
HD 68988 b	0.1249	1.86	0.0704	6.78	1.2
HD 73256 b	0.029	1.87	0.0371	0.83	1.05
HD 118203 b	0.309	2.14	0.0703	4.6	1.23
		3.0 to < 4.5 M_J			
HIP 14810 b	0.148	3.84	0.0692	···	0.99
τ Boo b	0.023	3.9	0.046	2.52	1.3

* transiting object

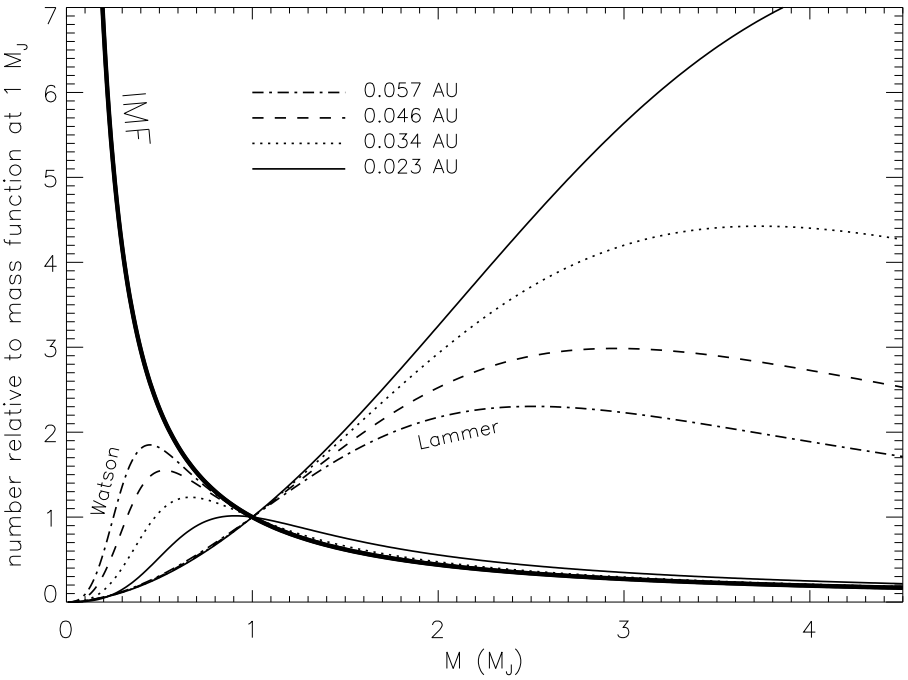

Fig. 1.— Predicted mass functions $f(M, t)$ for EGPs suffering mass loss over 5 Gyr, evaluated for four different orbital radii, using the Watson et al. (1981) escape rate (left-hand curves with maxima at masses between 0.4 M_J and 0.9 M_J), and the two-orders-of-magnitude larger Lammer et al. (2003) escape rate (right-hand curves with maxima at masses $\geq$ 2.3 M_J). The heavy curve (IMF) is the assumed mass distribution at the start of mass loss. All distributions are normalized to unity at $M = 1M_J$. See text for a more detailed discussion of this plot.

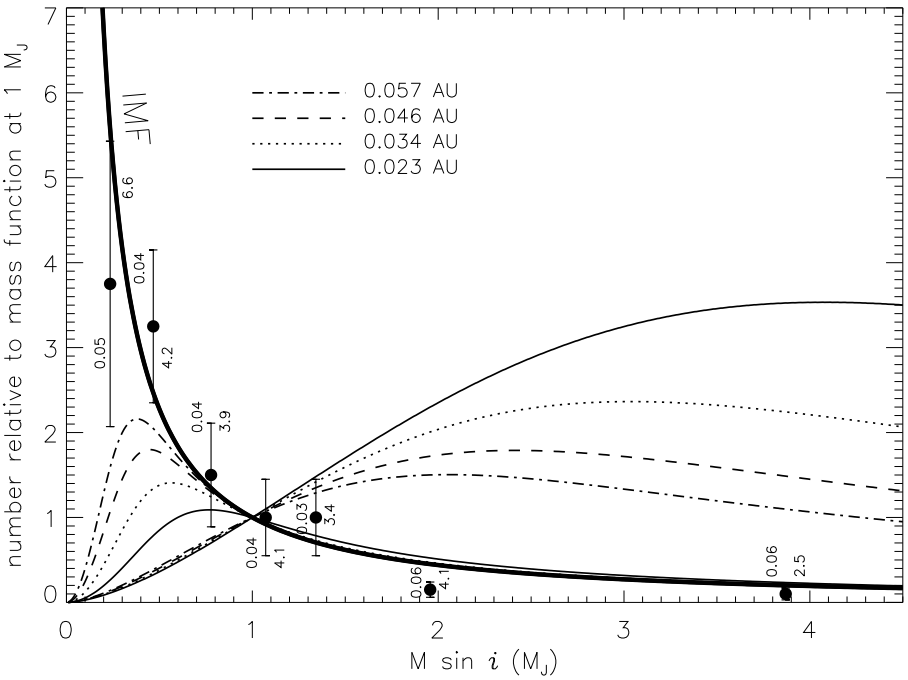

Fig. 2.— Predicted mass functions $g(M \sin i, t)$ for EGPs suffering mass loss over 5 Gyr, evaluated for the four different orbital radii and the two mass-loss models, compared with data for highly-irradiated EGPs. All distributions (theory and data) are normalized to unity at $M \sin i = 1\ M_J$. See text for a more detailed discussion of this plot.